Physica E 128 (2021) 114618

Contents lists available at ScienceDirect

Physica E: Low-dimensional Systems and Nanostructures

journal homepage: http://www.elsevier.com/locate/physe

Perovskite/InGaAs tandem cell exceeding 29% efficiency via optimizing spectral splitter based on RF sputtered ITO/Ag/ITO ultra-thin structure

H. Ferhati [a], F. Djeffal [a,*], A. Bendjerad [a], A. Benhaya [a], A. Saidi [b]

[a] LEA, Department of Electronics, University of Batna 2, Batna, 05000, Algeria
[b] Research Scientific and Technical Center on Physico-Chemical Analysis (CRAPC), Tipaza, Algeria

ARTICLE INFO

Keywords:
RF sputtering
Spectrum splitter
Multilayer
Tandem
Ultra-thin

ABSTRACT

In this paper, the optimization, elaboration and characterization of an efficient spectral beam splitter based on a simple RF sputtered ITO/Ag/ITO (IAI) ultra-thin multilayer structure are presented. An experimental investigation assisted by Genetic Algorithm (GA) metaheuristic optimization was carried out to achieve high-performance spectral splitter for tandem solar cell applications. The RF magnetron sputtering method was used to elaborate the optimized IAI structure. The optical and structural properties of the sputtered splitter were also analyzed using UV–Vis-IR spectroscopy and X-ray diffraction (XRD) measurements. It is found that the elaborated splitter structure offers 84% of transparency and a high reflectance of 87% with an optimum cut-off wavelength of 800 nm. This is attributed to the design approach, which leads to promote spectral splitting mechanism by inducing efficient optical modulation. Interestingly, a new Figure of Merit (FoM) parameter, which evaluates the optical splitting performances is proposed. Moreover, a new Perovskite/InGaAs tandem cell is proposed and analyzed to show the impact of the elaborated spectrum splitter on the solar cell efficiency. It is revealed that the investigated solar cell exhibits an improved efficiency approaching 30%. The latter value far surpasses that provided by Perovskite tandem cells. These results indicate that our spectrum splitting approach can open a new pathway towards designing high-performance tandem photovoltaic devices.

1. Introduction

Recently, the emergence of multi-junction technology at a reasonable cost has allowed a stunning progress in renewable energy resources [1–4]. Perovskite solar cells (PSCs) have attracted an enormous deal of attention to develop low-cost and high-efficiency tandem photovoltaic systems. This is due to the large flexibility, tunable band-gap and lower fabrication cost of perovskite materials [5–8]. Numerous Perovskite tandem architectures based on mechanically stacked or monolithically series-connected designs are proposed to achieve high absorption properties using different bottom-cells based on Silicon, GaAs, CIGS, Ge and CZTS materials [9–17]. However, the recorded efficiencies are still far from the expectations, where all forms of recombination, resistive and optical losses should be suppressed. Intuitively, combining $(FAPbI_3)_{0.95}(MAPbBr_3)_{0.05}$ Perovskite absorber showing 1.5eV band-gap with InGaAs narrow band-gap material (0.75eV) can offer a new pathway to develop efficient tandem SC, exhibiting a high photoresponse over the whole solar spectrum [18,19]. Therefore, this calls for a renewed performance assessment of Perovskite/InGaAs tandem photovoltaic device to potentially break the inherent limit associated with single-junction SCs. However, several undesired effects would be occurred when considering the latter tandem structure such as the need for complex interconnection layers, current matching condition, thermalization, lattice mismatching effects, optical and recombination losses that can drastically limit the multi-junction SC efficiency [15–19]. In addition, the bottom cell based on narrow band-gap materials generates much more current density leading to huge power dissipation as heat. This can in turn prevent maintaining low working temperatures, thus affecting the panel reliability against the degradation induced by heating effects. This becomes more severe when light concentrators are incorporated thereby reducing enormously the SC practical efficiency. Particularly, this effect is common for PSCs technology, where stability issues are more pronounced. One approach to avoid these undesired effects is to use spectral beam splitter technique, which has enabled higher efficiencies and regarded readily accessible to the photovoltaic industry [20–23].

The optical splitter separates the incident sun-light into some parts of spectral ranges and each part is directed to individual sub-cells whose

* Corresponding author.
E-mail address: faycal.djeffal@univ-batna2.dz (F. Djeffal).

https://doi.org/10.1016/j.physe.2020.114618
Received 30 August 2020; Received in revised form 12 December 2020; Accepted 30 December 2020
Available online 3 January 2021
1386-9477/

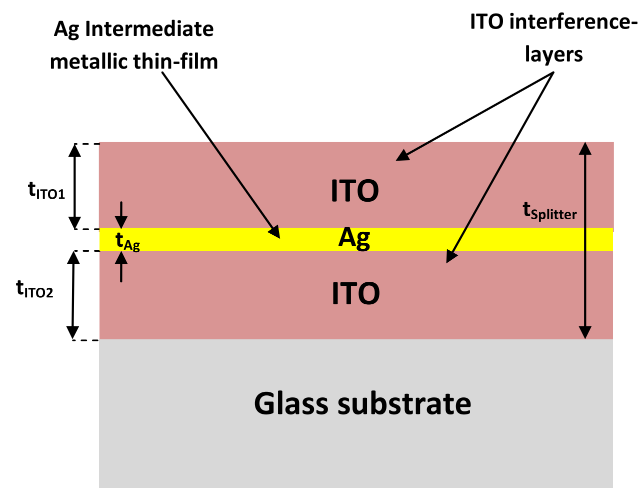

Fig. 1. Cross-sectional view of the proposed spectrum splitting system based on a simple IAI tri-layered structure.

band-gap energies correspond to the appropriate spectral range. Numerous splitting systems were proposed in the literature such as prismatic lens, dichroic coating and luminescence solar concentrator [20–28]. Nevertheless, it is still complex, sophisticated and time consuming to fabricate reliable and efficient beam splitter systems for tandem photovoltaics, where high number of interference layers is required to achieve suitable cut-off wavelength, reduced optical losses and sloped transition [24–26]. Accordingly, using adequate thin-film materials with reduced interference layers, while ensuring high splitting performances can open up the route for the elaboration of high-efficiency tandem SCs at low-cost. In this context, several multilayer-based structures have been developed for thermal-solar hybrid systems demonstrating a great promise in achieving suitable splitting characteristics and high energy harvesting performances [25–38]. However, they did not prove any benefit over the conventional ones in terms of cut-off wavelength tunability and optical properties. These effects make them too upstream to yet contemplate a potential deployment in tandem photovoltaic systems. To the best of our knowledge, no investigations based on a strategic combination between ITO/Ag/ITO (IAI) multilayer spectrum splitter and a new Perovskite/InGaAs tandem SC structure were conducted to achieve superior conversion efficiency at low-cost. To do so, in this paper, an experimental study assisted by systematic optimization approach was carried out for elaborating an efficient IAI multilayer structure. The optimized structure was prepared by RF magnetron sputtering technique and its optical and structural characteristics were analyzed using UV–Vis-IR and XRD measurements. It was revealed that the elaborated IAI multilayer spectrum-splitter exhibits 84% of transparency and a reflectance of 87% with an optimum cut-off wavelength of 800 nm, which has led to achieve a high-efficiency Perovskite/InGaAs tandem SC of 29.6%. Therefore, the proposed design and elaboration approaches not only provide promising techniques to optimize the performance of IAI multilayer spectrum-splitters by using metaheuristic methods, but also open up the way to develop high-efficiency tandem SCs.

2. IAI multilayer spectral beam splitter optimization and experimental procedure

This section is represented by two-stage investigation frameworks mainly dedicated to the design of novel simple spectrum splitter structure based on IAI tri-layers. Firstly, we present a new approach based on the strategic combination between Genetic Algorithm (GA) metaheuristic technique and Finite difference time domain (FDTD) method to identify the IAI geometry enabling efficient spectrum splitting performances for tandem photovoltaic applications. The second objective relies on elaborating and characterizing the optimized IAI tri-layered.

2.1. Structure and optimization

Spectrum splitter systems exhibiting sloped transition with suitable cut-off wavelength are highly attractive for developing efficient tandem SCs [21–26]. On the other hand, seeking alternative beam splitter structures involving a minimum number of interference layers is of paramount importance to reduce the elaboration cost and avoid processing complexity. To address this trade-off, the main idea behind the proposed design dwells on suggesting simple IAI tri-layer architecture. Fig. 1 shows the scheme of the investigated beam splitter structure. The proposed structure consists on stacking ITO, Ag and ITO thin-films on the glass substrate, where t_{ITO1}, t_{Ag} and t_{ITO2} represent their thickness, respectively. Ag conducting media is sandwiched between two ITO dielectric films to eventually modulate the structure optical behavior with the aim of designing effective and simple beam splitter. Moreover, the incidence angle α can induce significant changes concerning the IAI tri-layer optical performances, thus indicating its importance to ensure an appropriate light-scattering. For the modeling purposes, the Glass substrate thickness is represented by d_{Glass} and the entire thickness of the proposed splitter design is denoted as $t_{Splitter}$.

The proposed approach consists on combining FDTD method and GA optimization technique to identify the most favorable geometrical configuration of the proposed IAI multilayered structure, offering suitable optical performances for spectrum splitting applications. In this framework, the optical behavior of the investigated IAI tri-layers on glass substrate is modeled using SILVACO software [39]. In this tool, the associated optical parameters including transmittance, reflectance and absorbance are extracted using 2D-FDTD modeling approach, which is thoroughly detailed in our previous works [40,41]. Designing efficient and simple beam-splitters for multi-junction solar cell application through intuiting its structure and geometry is not sufficient to achieve the highest possible efficiencies. Otherwise, we believe that sophisticated global optimization techniques behaving like effective predictive simulations can give a great promise to identify the suitable IAI configuration for beam splitting applications. Thus, GA-based global optimization technique could principally transform the design step towards a search problem [42,43]. Moreover, taking into consideration the targeted splitting efficiency and the suitable cut-off wavelength yields an effective pathway to design simple, low-cost and high-performance light-splitters with minimal guesswork. To achieve this objective, the extracted optical parameters from 2-dimensional (2-D) FDTD are subsequently used to formulate the objective function of the GA global optimization approach. The latter optimization tool is effective, being able to deal with very complex multivariable mathematical issues. During the global optimization of GA, successive populations are generated using selection, crossover and mutation genetic operators. These parameters are applied to individuals within the population, enabling effectiveness for exploring areas in the search space to potentially identify the best combinations. This technique was extensively exploited to optimize various optoelectronic and nanoelectronic devices [43–46]. In our investigation, GA global optimization focuses on searching the appropriate geometry and the incident angle of the analyzed IAI tri-layer, allowing the efficient split of sunshine into two spectral ranges according to the potential application, where each part will be conveyed to a physically separated photovoltaic device tuned to properly matched band-gap absorber. In addition, the cut-off wavelength should be fixed in the fitness function with respect to the envisaged tandem application. Accordingly, the optimized IAI based beam splitter structure will be applied to outperform Perovskite/InGaAs double-junction solar cell, signifying that the cut-off wavelength should be fixed at 800 nm to harvest the maximum sun-light. Therefore, by considering a mono-objective global optimization scheme based on

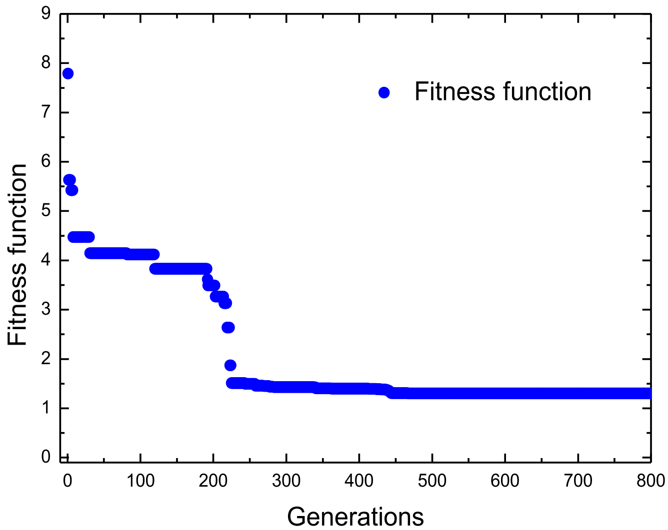

Fig. 2. Evolution of the fitness function against the number of generations associated with the performed GA optimization.

weighting coefficients, the fitness function is given by

$$Fitness(X_i) = w_1\left(\frac{1}{T[380nm, \lambda_{cut-off}]}\right) + w_2\left(\frac{1}{R[\lambda_{cut-off}, 1600nm]}\right) \quad (1)$$

where R and T are the average reflectance and transmittance within the considered spectral bands, $X_i = (t_{ITO1}, t_{ITO2}, t_{Ag}, \alpha)$of the i^{th}generation denotes the IAI tri-layer design parameter vector, w_1 and w_2 are weighting coefficients considered to be equal to 1/2. In order to get reasonable values according to the material consumption aspect and cost purposes, each design parameter is confined in a given range. These ranges are incorporated in the optimization procedure using the following constraint.

$\succ x_i \in [x_{m\min}, x_{m\max}],\ x_i \in X_i.$

It is worth mentioning that among various dielectric media such as ZnO, ZnS, ITO, NiO, WO_3 and TiO_2, ITO material is chosen because of its high-transparency over the visible spectrum range.

The population size and stall generation associated with the GA global optimization are taken respectively with 1000 and 20. Fig. 2 shows the variation of the objective function versus the number of GA generations. It can be observed from this figure that an excellent stabilization is achieved for 450 generations and the fitness function is appropriately minimized, thus proving the usefulness of the proposed systematic approach for designing efficient beam-splitter system. As a result, the IAI tri-layered design parameter vector is given by$X_i = (t_{ITO1} = 37nm, t_{ITO2} = 42nm, t_{Ag} = 20nm, \alpha = 49.5^\circ)$. Basically, the incident angle plays a crucial role in determining the light-matter interaction properties, where the variation of the incident angle can induce a complex optical behavior [47,48]. This is mainly due to the complex dependence of reflection, absorbance and transmission coefficients on several parameters including the layers thickness, material properties and angle of incidence associated with the investigated ITO/Ag/ITO multilayer-based spectrum splitter. The optimization procedure shows that the optimized IAI multilayer structure can offer a high transparency of 89% in the visible range, while maintaining a superior reflectance exceeding 91% over the NIR and IR bands. Moreover, the performed GA-based computation demonstrated that taking the incident angle with 49.5° could open up the way for reaching high-performance splitting characteristics of the incident light into two spectral ranges according to the potential application. This is due to the appropriateness of GA approach for selecting the best design parameters according to the defined fitness function, which is given by Eq. (1). These encouraging results prove its capability to split the solar spectrum into two parts with $\lambda_{cut\text{-}off} = 800$ nm, which emphasizes its great promise to be applied to enhance Perovskite/InGaAs tandem solar cell. Therefore, it seems of great importance to elaborate the optimized IAI-based beam splitter, which constitutes the main objective of the next sub-section.

2.2. Experiments

Experiments assisted by metaheuristic techniques can open up new routes for developing high-performance spectrum splitting systems

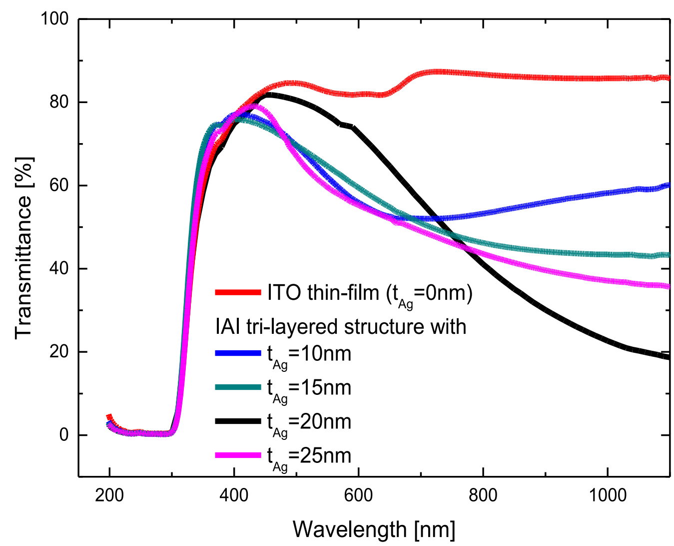

(a)

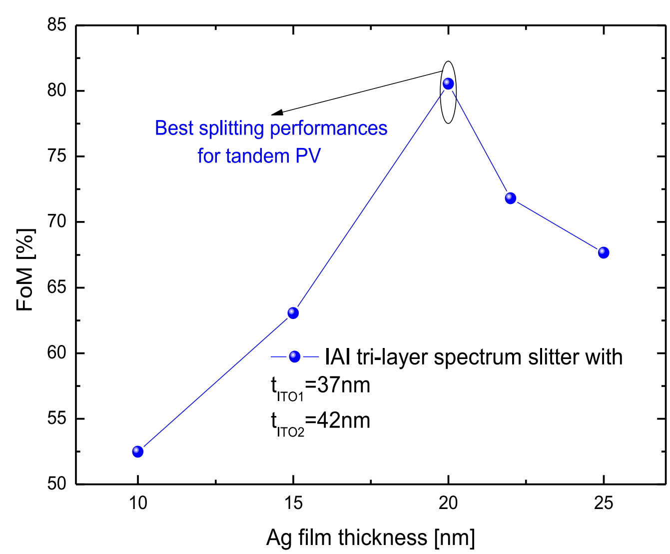

(b)

Fig. 3. (a) Transmittance spectra associated with the IAI multilayer optical filter with different intermediate Ag thickness values. **(b)** Variation of the FoM parameter as a function of intermediate Ag thickness of the investigated IAI-based spectrum splitter.

based on simple tri-layered structure for tandem photovoltaic applications. In this perspective, after selecting the optimized IAI multilayer geometry providing a high transparency below the cut-off frequency and superior reflectance above $\lambda_{cut\text{-}off}$ using the proposed systematic approach as it is thoroughly explained in the last sub-section, the next step is dedicated to the elaboration and the optical characterization of the optimized IAI tri-layer-based beam splitter structure. Before the deposition process of ITO and Ag interference sub-layers forming the optimized IAI multilayer spectrum splitter, Glass substrates were cleaned up using commercial detergent and the ultrasonic bath, where 10 min sequential sonication procedure in acetone, water and ethanol were carried out. Afterwards, the substrates were dried by using a nitrogen jet process. Subsequently, ITO and Ag interference thin-films with the optimized geometry (37nm/20nm/42 nm) were successively sputtered on the cleaned glass substrate using RF magnetron sputtering technique (MOORFIELD MiniLab 060), in which ITO target with 90 wt% In_2O_3 and 10 wt% SnO_2 and Ag targets with high purity of 99.99% were exploited. To show the strength of the proposed optimization approach and for comparison purposes, additional samples with different Ag intermediate thickness were also elaborated. Each sub-layer is separately deposited on a glass substrate first to optimize and to calibrate the RF sputtering procedure, enabling the elaboration of the optimized IAI trilayer spectrum splitter geometry with high accuracy. Accordingly, the thickness of the Ag and of ITO interference films was considered as it is outlined in section 2.1 for which the appropriate deposition rates were respectively 0.08 nm/s and 0.12 nm/s. The sputtering process of the stacked IAI multilayer was conducted in ambient conditions and in Ar and O_2 atmosphere (66% oxygen partial pressure) with a pressure of 1.5 Pa and 520W of source power. It is worth mentioning that the adopted RF magnetron sputtering experimental facility is widely exploited for the elaboration of high-quality ITO/Metal/ITO tri-layered structures [49–52]. This is mainly due to its capability for producing multilayers in a single technological cycle, exhibiting low contamination, high crystallinity and controllable thickness. These benefits offer exciting opportunities to achieve the predicted enhancements concerning the IAI spectrum splitting structure.

For the structural and optical characterizations, Ellipsometry measurement was carried out to determine and confirm the thickness of the prepared IAI tri-layered structure with optimized geometry. The structural properties of the elaborated samples were analyzed using X-Ray Diffraction (XRD) measurements (ARL Equinox 3000) for 2θ diffraction angle scans of [25°–80°]. The spectrophotometer (F10-RT-UV) was then exploited to extract the UV–Vis–NIR transmittance and reflection spectra of the fabricated IAI samples with dissimilar Ag intermediate layer thickness and that of the optimized structure.

3. Results and discussion

3.1. Optical and structural properties of the elaborated IAI multilayers

To elucidate the influence of the Ag conducting media geometry on the optical behavior of IAI tri-layered structure, Fig. 3 (a) illustrates the transmittance spectra associated with the prepared IAI multilayer samples with different silver interlayer thickness values ranging from 10 nm to 25 nm compared to that of the ITO thin-film. This figure demonstrates that inserting Ag ultrathin-film can reduce the transparency over the NIR range, which can be explained by the high-reflection effects induced by Ag material within this spectral range. It can be also seen that the variation of the Ag intermediate thickness induces a complex optical behavior, where the prepared IAI tri-layered structure exhibit a low transparency over the NIR range as compared to the ITO thin-film and maintains a high visible transmittance. This indicates the ability of the prepared IAI multilayer structure to serve as a simple low-cost spectrum splitter for tandem photovoltaics. In this perspective, to identify the most favorable IAI tri-layered structure enabling high-performance spectrum splitting, a new FoM parameter called splitter efficiency is proposed and can be given by the following formula

$$FoM = \left(\frac{T_{\max} - T_{\min}}{2}\right) + \left(\frac{R_{\max} - R_{\min}}{2}\right) \tag{2}$$

where T_{max} and T_{min} represent the maximum and minimum transparency, while R_{max} and R_{min} denote the maximum and minimum reflectance over the solar spectrum. It is worth mentioning that the perfect spectrum splitter exhibits 100% of FoM parameter.

The FoM parameter is calculated for all elaborated samples based on IAI multilayer structure. In this context, Fig. 3 (b) shows the variation of the FoM as a function of the silver intermediate layer thickness. It can be observed that the structure FoM increases with the silver intermediate film thickness increase from 52% for $t_{Ag} = 10$ nm to reach its maximum for $t_{Ag} = 20$ nm, offering a high splitting efficiency of 80.5%. After this optimum value, the FoM decreases with further increasing the Ag thinlayer thickness over 20 nm, where taking the Ag intermediate layer

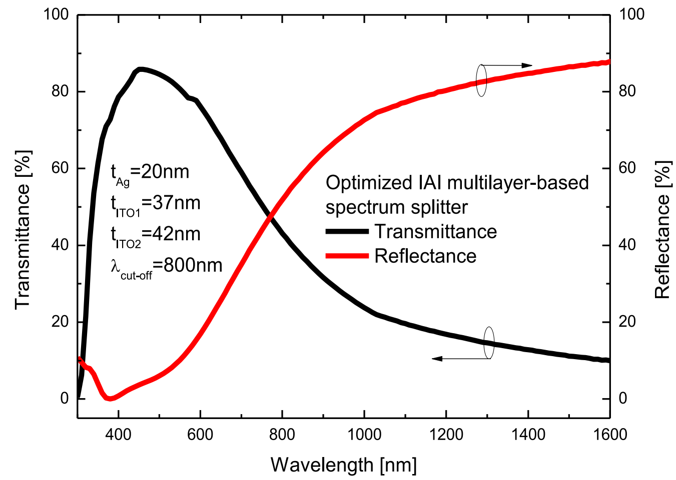

(a)

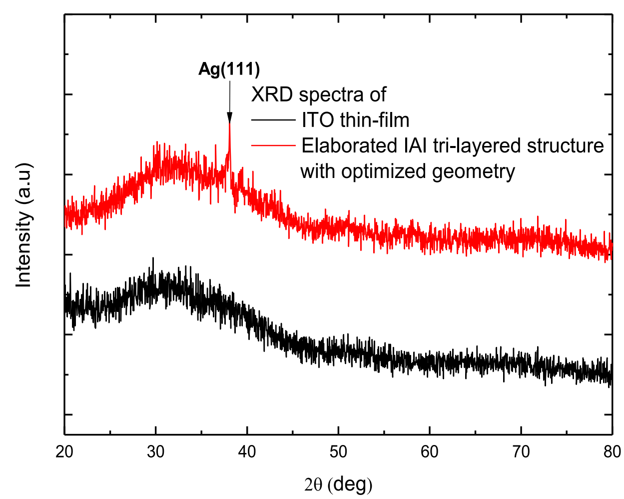

(b)

Fig. 4. (a) Transmittance and reflectance spectra associated with the elaborated spectrum splitter based on optimized IAI tri-layered structure with $\lambda_{cut-off} = 800$ nm. **(b)** XRD patterns associated with the elaborated IAI multilayer structure and that of the ITO thin-film.

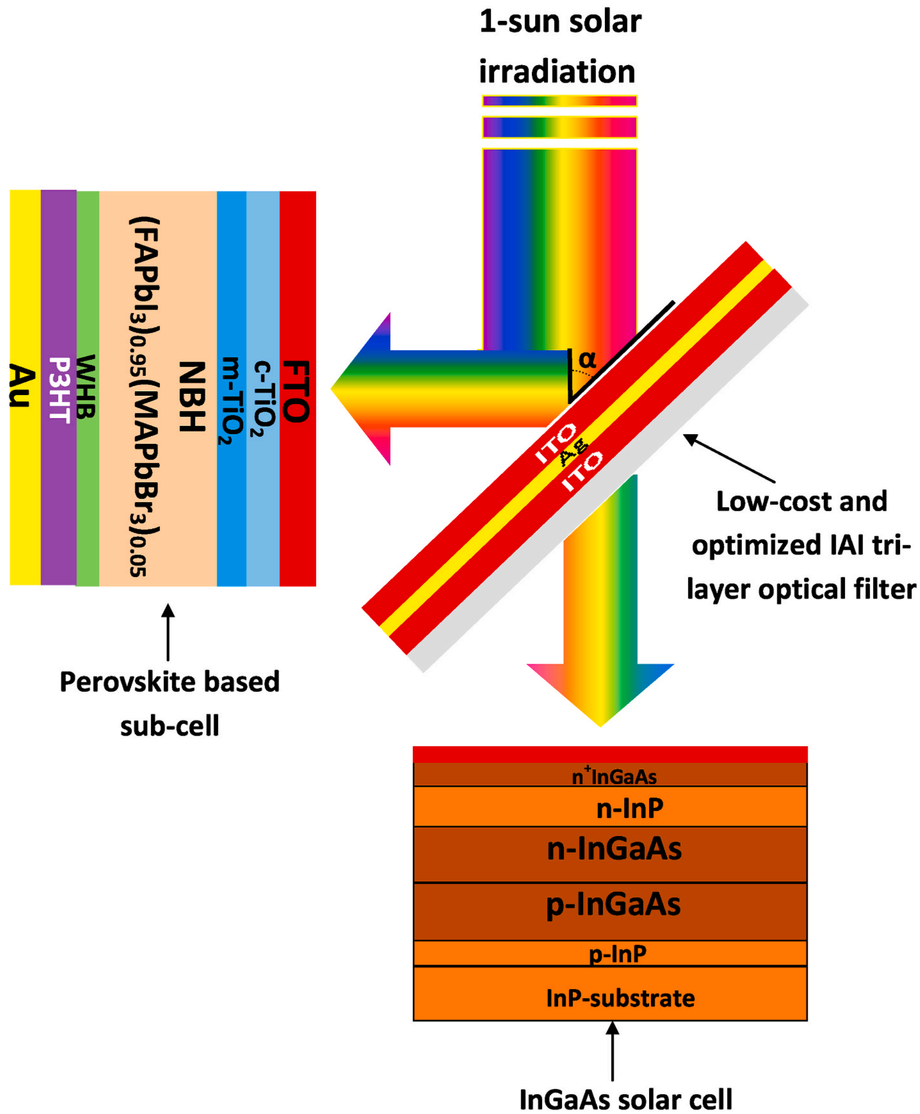

Fig. 5. Scheme of spectrum splitting system for Perovskite/InGaAs tandem architecture.

thickness with 25 nm leads to reduce the FoM parameter to the value of 67%. This emphasizes the complex optical behavior of the IAI multilayer structure, where the inserted Ag thin-layer induces interference effects leading to modulate the light-scattering behavior of the prepared structures. More importantly, the obtained results indicate the effectiveness of the adopted systematic optimization approach for providing efficient predictive simulation of the investigated IAI multilayer spectrum splitter, where a good agreement with the simulation results is recorded. In other words, the elaborated sample with the optimized tri-layer geometry (37nm/20nm/42 nm) has allowed reaching the highest splitting efficiency of 86%. In order to assess the capability of the prepared IAI multilayer with optimized structure for efficiently splitting the solar spectrum according to the envisaged application in Perovskite/InGaAs tandem photovoltaic device, Fig. 4 (a) depicts the transmittance and reflectance spectra associated with the elaborated IAI tri-layered beam splitter structure. Obviously, the fabricated structure demonstrates an excellent spectrum splitting performances at a cut-off wavelength of 800 nm, where it provides a maximum transparency of 85.8% with an average value of 70.7% within the spectrum band of [380 nm–800nm], while maintaining a superior reflectance exceeding 89% with an average value of 79.5% in the spectrum range of [800 nm–1600nm]. This confirms the capability of the IAI tri-layered structure for efficiently splitting the solar spectrum into two parts, which are regarded appropriate for Perovskite/InGaAs tandem photovoltaics using simple manufacturing process. This outstanding optical behavior is attributed to the proposed systematic approach based on experiments assisted by GA optimization technique for promoting an improved light-management leading to design high-performance spectrum splitter based on a simple and low-cost IAI multilayer structure. Despite the fact that the prepared IAI tri-layered structure has demonstrated a great promise in providing outstanding sunlight splitting characteristics, the transition from transmission to reflection is not perfect. This is attributed to the use of a simple structure involving only three interference layers. Otherwise, high number of interference layers is needed to achieve a perfectly sloped transition at a relatively low cut-off wavelength of 800 nm, which is time consuming and can impose the use of complicated manufacturing processes thereby increasing the elaboration cost of the spectrum splitting system. Accordingly, the main objective of our investigation is to make a good trade-off between the splitting efficiency and the overall fabrication cost, which can be fulfilled using an optimized and simple IAI tri-layered structure. Therefore, the next step is to assess the performance of the prepared beam splitter for Perovskite/InGaAs tandem solar cell, which constitutes the main goal of the subsequent sub-section (3.2).

The structural properties of the elaborated IAI tri-layered spectrum splitter are investigated using Fig. 4 (b). The latter figure shows XRD

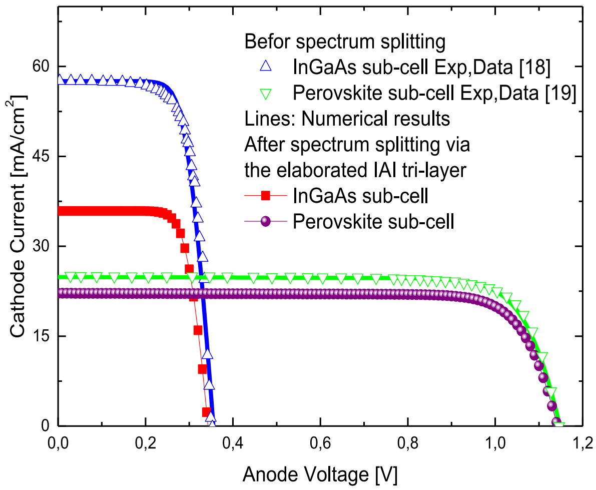

(a)

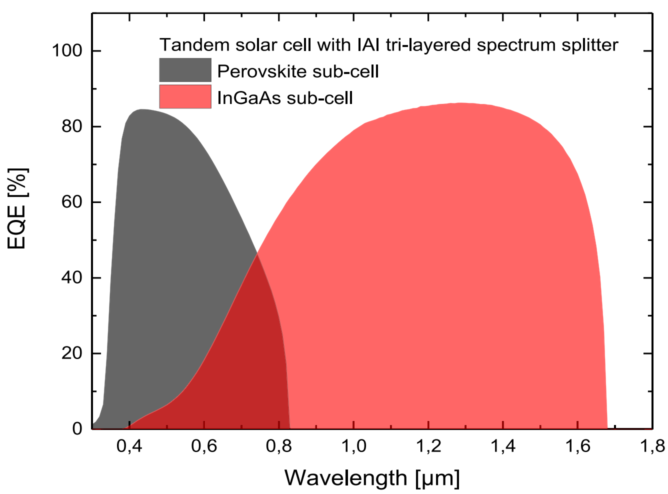

(b)

Fig. 6. (a) The I–V characteristics of the investigated Perovskite and InGaAs sub-cells with and without the elaborated spectrum splitting based on IAI multilayer. **(b)** EQE of both Perovskite and InGaAs top and bottom based solar cells.

patterns in the 2θ range from 20° to 80° of the sputtered IAI tri-layered structure and 60 nm thick ITO film on glass substrate. It is clearly seen from this figure that no coherent XRD peaks corresponding to the ITO material in both samples are observed, thus indicating the amorphous state of the sputtered films. This is mainly due to their ultrathin nature, where the thicknesses of the deposited ITO layers are not thick enough to reach the crystallization phase. On the other hand, this figure shows a small diffraction peak at 38° of 2θ position matching silver material from (111) hkl plane, proving the presence of an Ag layer at the beginning of crystallization phase. Markedly, these observations are found in accordance with diverse experimental investigations of sputtered IAI multilayer structures [49–52].

3.2. Implementation of sputtered IAI-based spectrum-splitter in tandem SCs

The outstanding splitting efficiency obtained from the prepared IAI tri-layer structure have inspired implementing it in a tandem photovoltaic device based on a new Perovskite/InGaAs double-junction architecture. The choice of the InGaAs sub-cell tandem partner is made according to the obtained fascinating splitting performances associated with the elaborated IAI multilayer structure, which exhibits a high transparency over the visible range and superior reflectance in the NIR and IR spectrum bands with an optimum cut-off wavelength of 800 nm. This indicates its potential for achieving highly enhanced sun-light harvesting performances. Accordingly, Fig. 5 describes the optimized spectrum splitting system based on simple sputtered IAI tri-layered structure acting as an optical filter, which is positioned at an incident angle $\alpha = 49.5^\circ$ to achieve suitable splitting efficiency as it is above-outlined. Basically, the cornerstone of our beam splitter system resides on conveying the transmitted light to the PSC, while the reflected sunlight from the IAI-based optical filter will be directed to the InGaAs sub-cell. Experimental sub-cells based on both Perovskite and InGaAs absorbers are used to show the role of the elaborated spectrum splitting structure in enhancing the photoconversion efficiency of the analyzed tandem device [18,19]. In this framework, InGaAs sub-cell is considered with n-type InP window, p-InP BSF back-layer and $In_{0.53}Ga_{0.47}As$ absorber with 0.74eV of band-gap. On the other hand, the adopted Perovskite sub-cell involves the use of consist $(FAPbI_3)_{0.95}(MAPbBr_3)_{0.05}$ absorber with 1.5eV band-gap energy. Besides, (n-i-p) perovskite sub-cell based on FTO/c-TiO_2/m-TiO_2/Perovskite/WHB/P3HT/Au structure is considered as it is described in Fig. 5.

Accurate analytical models developed in our previous works are used to extract the current-voltage characteristics of the InGaAs sub-cell [53], while the perovskite-based cell is analyzed using the Solar Cell Capacitance Simulator (SCAPS) [54]. The latter Simulator enables accurately modeling various technologies including Perovskite, crystalline and amorphous-based solar cells, demonstrating an outstanding capability for reproducing the experimental results [55–58]. The aim of this study is to elaborate a simple light-splitting technique to develop an efficient Perovskite/InGaAs tandem solar cell. To assess this hypothesis, the transmittance and reflection spectra provided by the UV–Vis-IR spectroscopy measurements were applied, respectively, to Perovskite and InGaAs sub-cells and the associated I–V curves are extracted. Fig. 6 (a) shows the I–V characteristics of the analyzed sub-cells with and without including the prepared IAI-based splitting system with optimized configuration compared to the experimental data of the sub-cells. It can be seen that the exploited solar cell models reproduce well the current dependence on the voltage, exhibiting a good agreement with the experimental results. After introducing the elaborated IAI multilayered spectrum splitter, the short-circuit current (I_{SC}) delivered by the InGaAs sub-cell is decreased from 57.6 mA/cm^2 under 1-sun illumination to 35.9 mA/cm^2. Similarly, the PSC cell generates an initial I_{SC} of 25 mA/cm^2, which is decreased to 22.4 mA/cm^2 after incorporating the sputtered IAI tri-layer-based splitter. These degradations are correlated to the optical losses induced by the introduced beam splitter system. To get a profound insight concerning the role of the spectrum splitter aspect on the tandem solar cell photoresponse characteristics, the External Quantum Efficiency (EQE) spectra of both InGaAs and Perovskite sub-cells are extracted and shown in Fig. 6 (b). It can be observed from this figure that photons with high energy are harvested by the PSC top cell with matched band-gap absorber of 1.5eV, where it shows a high-photoresponse over the visible spectrum range. Besides, the InGaAs sub-cell implemented in the spectrum splitting system demonstrates the ability for absorbing the incident light over the spectrum band of [780 nm–1600nm]. The EQE of the Perovskite/InGaAs tandem solar cell was found to be high in wide solar spectrum range of 350–1600 nm with a maximum value exceeding 83%. The sunlight absorption spectrum is extended to achieve 1600 nm due to the appropriate choice of the

Table 1
Overall photovoltaic performance comparison between the proposed Perovskite/InGaAs tandem solar cell based on the elaborated spectrum splitter with optimized IAI tri-layer structure and that of recently developed Perovskite-based tandem solar cells.

Photovoltaic solar cell configurations	I_{sc}[mA/cm^2]	V_{oc}[V]	FF [%]	Efficiency [%]
before spectrum splitting				
InGaAs solar cell [18]	57.6	0.35	71.3	14.4
Perovskite cell [19]	24.8	1.15	81.4	23.3
After spectrum splitting based on IAI multilayer structure				
InGaAs cell	2.4	0.34	73.8	9.2
Perovskite sub-cell	22.3	1.14	80	20.4
Perovskite-based Tandem structures				
2-T Perovskite/CZTS [9]	5.6	1.35	60.4	4.6
2-T Perovskite/CIGS [10]	18	1.59	75.7	21.6
4-T Perovskite/CIGS [11]	19.7	1.16	78.7	25
2-T Perovskite/c-Si [12]	14.7	1.78	80.4	21
4-T Perovskite/c-Si [13]	21.5	1.06	77.5	25.5
2-T Perovskite/GaAs [14]	14.3	2.16	78.8	24.3
4-T Perovskite/GaAs using optical splitter [14]	–	–	–	25.2
Perovskite/InGaAs with the IAI optimized spectrum splitting system (this work)	–	–	–	29.6

tandem partner and the splitting system cut-off wavelength. These outstanding results proves the effectiveness of the proposed systematic approach for promoting exciting opportunities to elaborated efficient optical filters allowing a high photoresponse over the whole solar spectrum.

For the completeness of this work, it appears significant to compare the photovoltaic performances of the developed Perovskite/InGaAs tandem device based on the elaborated IAI tri-layered spectrum splitting structure with recently fabricated Perovskite tandem solar cells [3–14]. Table .1 recapitulates the obtained photovoltaic parameters from the proposed Perovskite/InGaAs tandem SC and that of recently published results associated with 2-Terminal (2-T) and 4-T-based Perovskite double-junction SCs with dissimilar tandem partners with Silicon, CIGS, CZTS and GaAs absorbers. This table demonstrates that the proposed Perovskite/InGaAs tandem device with optimized IAI multilayer optical filter offers a high efficiency approaching 30% from the contribution of each sub-cell. The obtained value is much higher than that of the monolithically and mechanically stacked Perovskite tandem SCs reported in Refs. [9–14]. In addition, the use of a simple and high-performance optical filter carefully designed according to the potential application by the proposed systematic approach has allowed promoting reduced optical losses and avoiding all forms of degradations commonly encountered in tandem configuration such as recombination, thermalization, current-matching, requirement, lattice-mismatching and resistive effects. More importantly, the use of an efficient spectrum splitting system leads to suppress the PV thermal degradation effects, thus enabling the development of stable tandem solar cells offering high practical efficiencies. Therefore, we believe that the proposed systematic approach used to elaborate optimized built-in filters with suitably selected cut-off wavelength can be absolutely useful for designing high-efficiency tandem solar cells based on simple low-cost IAI tri-layered spectrum splitting systems.

4. Conclusion

In this work, a new systematic approach based on experiment assisted by GA global optimization technique is proposed to develop high-performance spectrum splitting system based on a simple low-cost IAI ultra-thin tri-layered structure. The latter structure is elaborated using RF magnetron sputtering method. XRD and UV–Vis-IR spectroscopy measurements were carried out and thoroughly discussed. A new FoM parameter describing the spectrum splitting performances is introduced. The influence of the Ag intermediate layer thickness on the splitting efficiency of the prepared samples is analyzed. It was revealed that high transparency of 84% and superior reflectance of 87% are respectively achieved in the spectral ranges below and above the cut-off wavelength value of 800 nm. More importantly, the sputtered IAI-based optical filter is implemented in a new Perovskite/InGaAs tandem architecture. The proposed SC structure demonstrates a high photoresponse over the entire solar spectrum with over than 83% of EQE. This result leads to record a high efficiency approaching 30%, far surpassing that of recently reported Perovskite-based tandem SCs. Therefore, offering such enhanced photoconversion efficiency, these innovative concepts of efficient cost-effective IAI tri-layer spectrum splitter system and carefully selected Perovskite tandem partner provide a sound strategy for the future development of the photovoltaic technology.

Declaration of competing interest

The authors declare that they have no known competing financial interests or personal relationships that could have appeared to influence the work reported in this paper.

References

[1] M. Jošt, L. Kegelmann, L. Korte, S. Albrecht, Monolithic perovskite tandem solar cells: a review of the present status and advanced characterization methods toward 30% efficiency, Advanced Energy Materials 10 (2020) 1904102.
[2] T.K. Todorov, D.M. Bishop, Y.S. Lee, Materials perspectives for next-generation low-cost tandem solar cells, Sol. Energy Mater. Sol. Cell. 180 (2018) 350–357.
[3] H. Ferhati, F. Djeffal, Exceeding 30% efficiency for an environment-friendly tandem solar cell based on earth-abundant Se/CZTS materials, Phys. E Low-dimens. Syst. Nanostruct. 109 (2019) 52–58.
[4] F. Hou, C. Han, O. Isabella, L. Yan, B. Shi, J. Chen, S. An, Z. Zhou, W. Huang, H. Ren, Q. Huang, G. Hou, X. Chen, Y. Li, Y. Ding, G. Wang, C. Wei, D. Zhang, M. Zeman, Y. Zhao, X. Zhang, Inverted pyramidally-textured PDMS antireflective foils for perovskite/silicon tandem solar cells with flat top cell, Nanomater. Energy 56 (2019) 234–240.
[5] Z. Zhang, Z. Li, L. Meng, S.-Y. Lien, P. Gao, Perovskite-based tandem solar cells: get the most out of the sun, Adv. Funct. Mater. 131 (2020) 2001904.
[6] S. Nair, S.B. Patel, J.V. Gohel, Recent trends in efficiency-stability improvement in Perovskite solar cells, Materialstoday Energy 17 (2020) 100449.
[7] M.A. Green, E.D. Dunlop, J. Hohl-Ebinger, M. Yoshita, N. Kopidakis, A.W.Y. Ho-Baillie, Solar cell efficiency tables (Version 55), Prog. Photovoltaics Res. Appl. 28 (2020) 3–15.
[8] Q. Tai, K.-C. Tang, F. Yan, Recent progress of inorganic perovskite solar cells, Energy Environ. Sci. 12 (2019) 2375–2405.
[9] T. Todorov, T.S. Gershon, O. Gunawan, S. Guha, Perovskite-kesterite monolithic tandem solar cells with high open-circuit voltage, Appl. Phys. Lett. 86 (2014) 173902–182106.
[10] M. Jošt, et al., 21.6%-Efficient monolithic perovskite/Cu(in,Ga)Se2 tandem solar cells with thin conformal hole transport layers for integration on rough bottom cell surfaces, ACS Energy Letter 4 (2019) 583–590.
[11] S. Gharibzadeh, et al., "2D/3D heterostructure for semitransparent perovskite solar cells with engineered bandgap enables efficiencies exceeding 25% in four-terminal tandems with silicon and CIGS, Adv. Funct. Mater. 30 (2020) 1909919.
[12] C.O.R. Quiroz, et al., Interface molecular engineering for laminated monolithic perovskite/silicon tandem solar cells with 80.4% fill factor, Adv. Funct. Mater. 29 (2019) 1901476.
[13] H.A. Dewi, et al., Highly efficient semitransparent perovskite solar cells for four terminal perovskite-silicon tandems, ACS Appl. Mater. Interfaces 27 (2019) 34178–34187.
[14] Zijia Li, et al., Wide-Bandgap perovskite/gallium arsenide tandem solar cells, Adv. Energy Mater. 10 (2020) 1903085.
[15] T. Todorov, et al., Monolithic perovskite-CIGS tandem solar cells via in situ band gap engineering, Adv. Energy Mater. 5 (2015) 1500799.
[16] W. Zi, X. Ren, X. Ren, Q. Wei, F. Gao, S.F. Liu, Perovskite/germanium tandem: a potential high efficiency thin film solar cell design, Optic Commun. 380 (2016) 1–5.
[17] Z. Song, et al., Wide-bandgap, low-bandgap, and tandem perovskite solar cells, Semicond. Sci. Technol. 34 (2019), 093001.
[18] Y.-C. Kao, et al., "Performance comparison of III–V//Si and III–V//InGaAs multijunction solar cells fabricated by the combination of mechanical stacking and wire bonding", Sci. Rep. 9 (2019) 1–9.
[19] E.H. Jung, et al., Efficient, stable and scalable perovskite solar cells using poly(3-hexylthiophene), Nature 567 (2019) 511–515.
[20] D. Lan, M.A. Green, The potential and design principle for next-generation spectrum-splitting photovoltaics: targeting 50% efficiency through built-in filters and generalization of concept, Prog. Photovoltaics Res. Appl. 27 (2018) 1–8.

[21] C. Maragliano, H. Apostoleris, M. Bronzoni, S. Rampino, M. Stefancich, M. Chiesa, Efficiency enhancement in two-cell CIGS photovoltaic system with low-cost optical spectral splitter, Optic Express 24 (2016) 222–233.
[22] F. Cao, Y. Huang, L. Tang, T. Sun, S.V. Boriskina, G. Chen, Z. Ren, Toward a high-efficient utilization of solar radiation by quad-band solar spectral splitting, Adv. Mater. 2r (2016) 10659–10663.
[23] C.N. Eisler, et al., The polyhedral specular reflector: a spectrum-splitting multijunction design to achieve ultrahigh (>50%) solar module efficiencies, IEEE Journal of Photovoltaics 9 (2019) 174–182.
[24] A. Mojiri, R. Taylor, E. Thomsen, G. Rosengarten, "Spectral beam splitting for efficient conversion of solar energy—a review, Renew. Sustain. Energy Rev. 28 (2013) 654–663.
[25] J.S.Q. Liu, R.A. Pala, F. Afshinmanesh, W. Cai, M.L. Brongersma, A submicron plasmonic dichroic splitter, Nat. Commun. 2 (2011) 525.
[26] W. Jiachen, S.B. Lee, K. Lee, Design of broadband multilayer dichroic coating for a high-efficiency solar energy harvesting system, Appl. Optic. 54 (2015) 4805–4811.
[27] D.-W. Kang, Y. Takiguchi, P. Sichanugrist, M. Konagai, InGaP//GaAs//c-Si 3-junction solar cells employing spectrum-splitting system, Prog. Photovoltaics Res. Appl. 24 (2016) 1016–1023.
[28] S. Kim, S. Kasashima, P. Sichanugrist, T. Kobayashi, T. Nakada, M. Konagai, Development of thin-film solar cells using solar spectrum splitting technique, Sol. Energy Mater. Sol. Cell. 119 (2013) 214–218.
[29] E.J.H. Skjølstrup, T. Søndergaard, Design and optimization of spectral beamsplitter for hybrid thermoelectric-photovoltaic concentrated solar energy devices, Sol. Energy 139 (2016) 149–156.
[30] K.P. Sibin, N. Selvakumar, A. Kumar, A. Dey, N. Sridhara, H.D. Shashikala, A. K. Sharma, H.C. Barshilia, Design and development of ITO/Ag/ITO spectral beam splitter coating for photovoltaic-thermoelectric hybrid systems, Sol. Energy 141 (2017) 118–126.
[31] S.H. Yu, C.H. Jia, H.W. Zheng, L.H. Ding, W.F. Zhang, High quality transparent conductive SnO2/Ag/SnO2 tri-layer films deposited at room temperature by magnetron sputtering, Mater. Lett. 85 (2012) 68–70.
[32] S.H. Yu, W. Zhang, L. Li, D. Xu, H. Dong, Y. Jin, Transparent conductive Sb-doped SnO2/Ag multilayer films fabricated by magnetron sputtering for flexible electronics, Acta Mater. 61 (2013) 5429–5436.
[33] S.H. Yu, W. Zhang, L. Li, D. Xu, H. Dong, Y. Jin, Optimization of SnO2/Ag/SnO2 tri-layer films as transparent composite electrode with high figure of merit, Thin Solid Films 552 (2014) 150–154.
[34] S.H. Yu, L. Li, D. Xu, H. Dong, Y. Jin, Investigation of low resistance transparent F-doped SnO2/Cu bi-layer films for flexible electronics, Vacuum 102 (2014) 43–47.
[35] S. Yu, L. Li, D. Xu, H. Dong, Y. Jin, Characterization of SnO2/Cu/SnO2 multilayers for high performance transparent conducting electrodes, Thin Solid Films 562 (2014) 501–505.
[36] S.H. Yu, L. Li, X. Lyu, W. Zhang, Preparation and investigation of nano-thick FTO/Ag/FTO multilayer transparent electrodes with high figure of merit, Sci. Rep. 6 (2016) 20399.
[37] S.H. Yu, Y. Liu, H. Zheng, L. Li, Y. Sun ", Improved performance of transparent-conducting AZO/Cu/AZO multilayer thin films by inserting a metal Ti layer for flexible electronics, Optic Lett. 42 (2017) 3020–3023.
[38] S. Yu, H. Zheng, L. Li, S. Chen, Highly conducting and transparent antimony doped tin oxide thin films: the role of sputtering power density, Ceram. Int. 43 (2017) 5654–5660.
[39] Atlas User's Manual, SILVACO TCAD, 2012.
[40] H. Ferhati, F. Djeffal, New high performance ultraviolet (MSM) TiO2/glass photodetector based on diffraction grating for optoelectronic applications, Optik 127 (2016) 7202–7209.
[41] H. Ferhati, F. Djeffal, A novel high-performance self-powered ultraviolet photodetector: concept, analytical modeling and analysis, Superlattice. Microst. 112 (2017) 480–492.
[42] C. Blum, A. Roli, Metaheuristics in combinatorial optimization: overview and conceptual comparison, ACM Comput. Surv. 35 (2003) 268–308.
[43] S. Fidanova, O. Roeva, Metaheuristic techniques for optimization of an E. coli cultivation model, Biotechnol. Biotechnol. Equip. 27 (2013) 3870–3876.
[44] F. Djeffal, H. Ferhati, T. Bentrcia, Improved analog and RF performances of gate-all-around junctionless MOSFET with drain and source extensions, Superlattice. Microst. 90 (2016) 132–140.
[45] H. Ferhati, F. Djeffal, N. Martin, Highly improved responsivity of self-powered UV-Visible photodetector based on TiO2/Ag/TiO2 multilayer deposited by GLAD technique: effects of oriented columns and nano-sculptured surface, Appl. Surf. Sci. 529 (2020) 147069.
[46] H. Ferhati, F. Djeffal, Role of gradual gate doping engineering in improving phototransistor performance for ultra-low power applications, J. Comput. Electron. 15 (2016) 550–556.
[47] M. Sadman, S. Rahman, M. Kawsar Alam, ", Effect of angle of incidence on the performance of bulk heterojunction organic solar cells: a unified optoelectronic analytical framework, AIP Adv. 7 (2014), 065101.
[48] X. Zhao, R. Xia, H. Gu, X. Ke, Y. Shi, X. Chen, H. Jiang, H.-L. Yip, S. Liu, Performance optimization of tandem organic solar cells at varying incident angles based on optical analysis method, Optic Express 28 (2020) 2381–2397.
[49] M. Girtan, Comparison of ITO/metal/ITO and ZnO/metal/ZnO characteristics as transparent electrodes for third generation solar cells, Sol. Energy Mater. Sol. Cells 100 (2012) 153–161.
[50] W. Wei, R. Hong, J. Wang, C. Tao, D. Zhang, Electron-beam irradiation induced optical transmittance enhancement for Au/ITO and ITO/Au/ITO multilayer thin films, J. Mater. Sci. Technol. 33 (2017) 1107–1112.
[51] S.Y. Lee, Y.S. Park, T. Seong, Optimized ITO/Ag/ITO multilayers as a current spreading layer to enhance the light output of ultraviolet light-emitting diodes, J. Alloys Compd. 776 (2019) 960–964.
[52] S.H. Park, S.M. Lee, E.H. Ko, T.H. Kim, Y.C. Nah, S.J. Lee, J.H. Lee, H.K. Kim, Roll-to-Roll sputtered ITO/Cu/ITO multilayer electrode for flexible, transparent thin film heaters and electrochromic applications, Sci. Rep. 6 (2016) 33868.
[53] H. Ferhati, F. Djeffal, Graded band-gap engineering for increased efficiency in CZTS solar cells, Opt. Mater. 76 (2018) 393–399.
[54] SCAPS Manual, Version, 29 december 2016.
[55] A. Ahmed, K. Riaz, H. Mehmood, T. Tauqeer, Z. Ahmad, Performance optimization of CH3NH3Pb(I1-xBrx)3 based perovskite solar cells by comparing different ETL materials through conduction band offset engineering, Opt. Mater. 105 (2020) 109897.
[56] S. Rai, B.K. Pandey, D.K. Dwivedi, Modeling of highly efficient and low cost CH3NH3Pb(I1-xClx)3 based perovskite solar cell by numerical simulation, Opt. Mater. 100 (2020) 109631.
[57] U. Saha, M.K. Alam, Proposition and computational analysis of a kesterite/kesterite tandem solar cell with enhanced efficiency, RSC Adv. 7 (2017) 4806.
[58] I.D.L. Santos, et al., Optimization of $CH_3NH_3PbI_3$ perovskite solar cells: a theoretical and experimental study, Sol. Energy 199 (2020) 198–205.